Phosphorylated MCM-22 Supported CeO_2-ZrO_2 Nanosphere Catalyst with Strong Anti-$PbCl_2$ Ability for NH_3-SCR

Xinyu Han[1, 2, a], Kaijie Liu[1, 2, b], Daying Zheng[1, 2, c], Xin Yang[1, 2, d], Yibo Zhang[1, 2, e,*1]

[1]Ganjiang Innovation Academy/Jiangxi Institute of Rare Earths, Chinese Academy of Sciences, No.1, Science Academy Road, Ganzhou 341000, China.
[2] School of Rare Earths, University of Science and Technology of China, Hefei 230041, China;

ABSTRACT

The flue gases emitted from boilers such as waste incineration plants and thermal power plants often contain a certain amount of Pb. This Pb can cause the NH_3-SCR catalyst to deactivate, thereby increasing NOx emissions. To address this issue, phosphorylated MCM-22 was used as the support for CeO_2-ZrO_2 nanospheres to synthesize CZMP catalysts with strong Pb poisoning resistance. These catalysts were able to purify more than 80% of NOx at a temperature of 300 °C after Pb poisoning. X-ray diffraction, powder FT-IR, and TEM analyses revealed that the structure and composition of the catalyst is stable and unchanged before and after Pb poisoning. NH_3-TPD result showed that phosphoric acid modification could change the acidity of the catalyst and H_2-TPR indicated the increase of low temperature redox sites, enhancing its anti-poisoning ability at low temperatures. In-situ DRIFT studies indicated that phosphoric acid modification caused rapid decomposition of nitrate intermediates on the catalysts, with the reaction dominated by an E-R mechanism.

Keywords: Nanosphere; CeO_2 catalyst; Zeolite; Pb poison; NH_3-SCR; Rare earth.

1. INTRODUCTION

Nitrogen oxides (NOx) have been identified by environmental research institutions worldwide as air pollutants posing serious risks.[1, 2] Among the commonly used NOx gas purifying method is selective catalytic reduction (SCR) using NH_3, which is efficient already in commercial use.[3] However, flue gas from some solid waste incineration plants and thermal power plants contains ash rich in heavy metal lead (Pb). This Pb can occupy the acid site of the catalyst, block its pores, and destroy its redox sites, ultimately deactivating the catalyst.[4] Several commercially available V_2O_5-WO_3/TiO_2 (VWTi) catalysts and Ce-based catalysts are believed to be ineffective in the presence of Pb poisoning.[5] Therefore, research on catalyst Pb poisoning has made strides. For example, Zou et al. synthesized Pb-poisoned CeO_2-WO_3/TiO_2 NH_3-SCR catalysts that converted 80% of NOx at 300 °C.[6] Similarly, Jiang et al. prepared CeO_2-WO_3/TiO_2 via another method and found that their catalyst could purify more than 70% of NOx at 350 °C.[7]

We believe that the anti-poisoning ability of Pb can be improved by adjusting the number and distribution of acidic sites. In this paper, phosphoric acid was used to modify MCM-22 molecular sieve as a support for CeO_2-ZrO_2 nanospheres to regulate the acid sites of catalyst through reasonable acidification and reduce the Pb-occupied acidic sites. Many characterization methods, including X-ray diffraction (XRD), chemisorption test (NH_3-TPD, H_2-TPR) and In-situ DRIFTs techniques were used to study the physical and chemical properties of the catalysts after Pb poisoning. Test results showed that the catalyst exhibited excellent SCR performance and anti-poisoning ability.

[1] [a] xinyuhan@mail.ustc.edu.cn, [b] liukaijie@gia.cas.cn, [c] dayingz@mail.ustc.edu.cn, [d] yxupupup@mail.ustc.edu.cn, [e*] yibozhang@gia.cas.cn

The International Conference Optoelectronic Information and Optical Engineering (OIOE2024), edited by Yang Yue, Lu Leng, Proc. of SPIE Vol. 13513, 135132I · © 2025 SPIE · 0277-786X · © The Authors.
 · doi: 10.1117/12.3045720

2. EXPERIMENTAL

2.1 Catalyst preparation

Phosphorylation of MCM-22. 1 g MCM-22 was added to 40 mL 0.04 mol/L $(NH_3)_2HPO_4$ solution. The mixture was then stirred at 25 °C for 24 h. The suspension would dry directly at 80 °C without centrifugation. The solid was subsequently heated by a muffle furnace at 120 °C for 4 h and 540 °C for 6 h.

Synthesis of Zr-doped CeO_2 nanospheres. The monodisperse Zr-doped CeO_2 nanospheres were obtained by hydrothermal method. Firstly, 0.18 mmol $Ce(NO_3)_3 \cdot 6H_2O$ and 0.02 mmol $Zr(NO_3)_4 \cdot 5H_2O$ were dissolved with 40 mL ethanol. When the two nitrates are all dissolved, 0.8 g PVP was added into the solution. Then, 0.415 mL triethylamine was slowly added dropwise to it. After stirring of 10 min, the lightly yellow mixture was poured into a 100 mL teflon-lined in stainless-steel autoclave. The vessel was put into a insulated container and heated at 180 °C for 24 h. The CeO2 nanospheres were dispersed into colloid homogeneously.

Load Zr-doped CeO_2 nanospheres on MCM-22 support. 40 mL of the Zr-doped CeO_2 nanospheres colloid was added into a crucible, and 0.301 g support was added in the crucible. The mixture was then stirred at 80 °C and evaporated to dryness. Then the crucible was placed in a muffle furnace and heated to 500 °C for 4 h. The catalyst with MCM-22 as the support was named CZM, and the catalyst with phosphoric acid modified MCM-22 as the support was named CZMP.

PbCl2 poisoning of catalysts. 0.003g $PbCl_2$ was dispersed in 50 mL deionized water in a crucible. Then 0.297 g catalyst was added into the crucible. Whereafter, the mixture was stirred at 90 °C and evaporated to dryness. Then the crucible was placed in a muffle furnace at 500 °C for 4 h.

2.2 Measurement of NH3-SCR performance

A self-made fixed bed reactor equipped with heater was used as the testing device for NH_3-SCR performance. The gases tested contained NO (500 ppm), NH_3 (500 ppm), O_2 (5%) and Ar in balance. The catalyst would be heated from room temperature to 350 °C. The gas content data collection began at 200 °C and ended at 350 °C. 83.3 mg of catalyst was weighed and put in a quartz tube, and the NH_3-SCR reactions were carried out at a space velocity of 60,000 mL/(g·h). The outlet contents of NH_3, NO, NO_2, and N_2O were detected using a Thermo Fisher IGS Analyzer. All of the results were recorded, and NOx conversion was summarized using the following eq. (1), while N_2 selectivity was calculated using eq. (2):

$$\mathrm{NO_x\ conversion\ (\%)} = \left(1 - \frac{[\mathrm{NO}]_{\mathrm{out}} + [\mathrm{NO_2}]_{\mathrm{out}}}{[\mathrm{NO}]_{\mathrm{in}} + [\mathrm{NO_2}]_{\mathrm{in}}}\right) \times 100\% \quad (1)$$

$$\mathrm{N_2\ selectivity\ (\%)} = \left(1 - \frac{2[\mathrm{N_2O}]_{\mathrm{out}}}{[\mathrm{NO_x}]_{\mathrm{in}} + [\mathrm{NH_3}]_{\mathrm{in}} - [\mathrm{NO_x}]_{\mathrm{out}} - [\mathrm{NH_3}]_{\mathrm{out}}}\right) \times 100\% \quad (2)$$

Where, [NOx]in and $[NH_3]$in is the inlet concentration (ppm) of NO + NO_2 and NH_3 of the reactor. [NOx]out, $[NO_2]$out and $[N_2O]$out represent gas concentration from the exit of the reactor of NO + NO_2, NO_2 and N_2O from the reactor.

2.3 Characterization

X-ray powder diffraction (XRD) patterns of catalysts were obtained using a D8 Advance XRD instrument from Bruker. The FT-IR tests were carried out on the iS50 FT-IR spectrometer from Thermo Scientific equipped with an ATR powder spectral test device. Transmission electron microscope (TEM) images were taken using a CCD camera on Talos F200x from FEI. The temperature programmed desorption of NH_3 (NH_3-TPD) and temperature programmed reduction of H_2 (H_2-TPR) experiments were performed on a Micromeritics Autochem II 2920 chemisorption instrument. The composition of the catalyst is tested by X-ray fluorescence (XRF) analysis, the instrument used is ZSX Primus III+ spectrometer. In-situ DRIFT measurements were performed using a Nicolet iS50 FT-IR spectrometer at the IR wavenumber ranging from 4000 to 650 cm^{-1} with a DRIFTs sample cell from Harrick and an MCT detector by accumulating 32 scans.

3. RESULT AND DISCUSSION

3.1 Phase and morphology

X-ray diffraction (XRD) is a widely used technique to analyze the structure of substances. In this study, XRD was employed to investigate the phase changes before and after modification with MCM-22 and CeO2-ZrO2 loading. The results are presented in Fig. 1(a) and Fig. 1(b), which depict the XRD patterns of the standard MCM-22 and the modified samples, respectively. From the XRD patterns, it can be observed that the diffraction peak of CZMP remains unchanged compared to the standard MCM-22 card. This indicates that the phosphoric acid modification did not destroy the structure

of MCM-22, and it still maintains a relatively complete structure. Additionally, the peaks of the nanospheres on the catalyst can be identified, confirming successful loading of these nanospheres onto the MCM-22 molecular sieve. Comparing the XRD patterns of PbCZM and PbCZMP, it was found that Pb poisoning had minimal impact on the structure of MCM-22. However, Pb poisoning significantly reduced the intensity of CeO_2 diffraction peaks on PbCZMP, suggesting that some of the nanospheres were redispersed or transformed into other substances. The FT-IR spectrum of these catalysts is presented in Fig. 1(c). By comparing the spectra before and after poisoning, it can be observed that the vibration absorption peak of SiO_2 skeleton in MCM-22 at 1050 cm^{-1} does not change significantly. This further confirms that the catalyst maintains structural stability even after Pb poisoning. Fig. 1(c) to Fig. 1(g) are TEM photos of catalysts of CZM, CZMP, PbCZM and PbCZMP. As depicted in the TEM images, the nanospheres have a diameter of approximately 6 nm and are uniformly distributed on the MCM-22 molecular sieve. Despite being poisoned, the morphology of the MCM-22 remains flake-like. It is noteworthy that the TEM image of PbCZMP display more black spots compared to other catalysts, which indicates that the aggregation of the nanospheres remains unchanged, but their properties may have undergone changes. Furthermore, XRF technology is employed to ascertain the composition and content of the catalyst. The results of the XRF test are presented in Table 1. From the table, it can be deduced that the loading percentage of nanospheres onto the catalyst is approximately 10%. Simultaneously, the PbO concentration in PbCZM is only 0.44%, which can be attributed to the partial oxidation of $PbCl_2$.

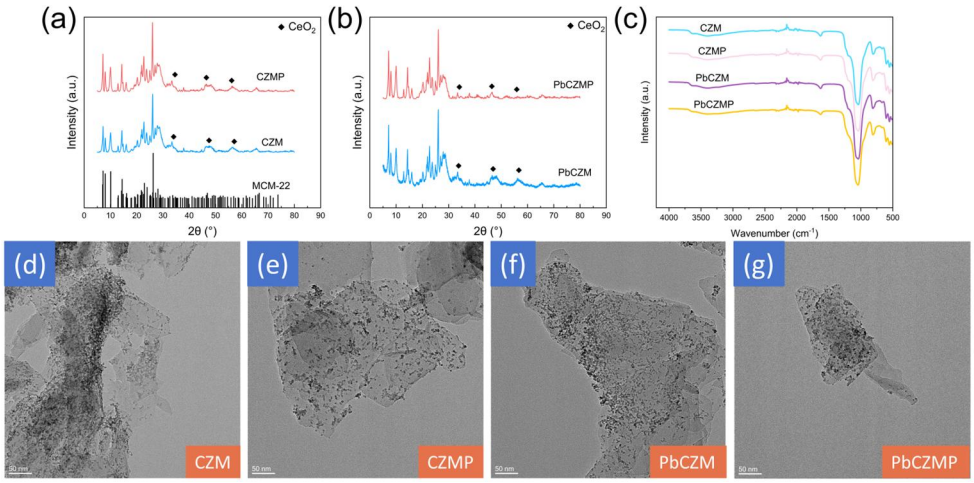

Figure. 1 (a) and (b) XRD patterns, (c) FT-IR spectra of catalysts before and after Pb poisoning. Panes (d) to (g) are TEM images of catalysts before and after Pb poisoning.

Table 1. Mass percentage of several oxides of catalysts before and after Pb poisoning by XRF.

Materials	Al_2O_3 (%)	SiO_2 (%)	Si/Al ratio	CeO_2 (%)	PbO (%)
CZM	5.2	82.1	15.91	11.8	
CZMP	4.8	76.3	15.83	12.9	
PbCZM	5.4	82.0	15.30	11.4	0.44
PbCZMP	4.6	70.1	15.27	15.7	1.58

3.2 NH_3-SCR performance

Fig. 2(a) shows the SCR performance of the catalyst at different temperatures from 200 to 350 °C. It be seen from the figure, CZM converts more than 90% of NOx at 250 °C and 300 °C, but after poisoning, it decreases from 80% to 20% of NOx conversion at 350 °C. However, CZMP and PbCZMP have satisfactory SCR performance. Whether it is poisoned or not, this catalyst can purify more than 90% of NOx at 250 to 350 °C. The N_2 selectivity of the catalyst was shown in Fig. 2(b). From the figure, it can be found that the selectivity of all catalysts is higher than 80%, which indicates that only little N_2O was produced in the reaction. At the same time, after 250 °C, the N_2 selectivity before Pb poisoning was much higher than that after poisoning, indicating that Pb poisoning affected the redox ability of the catalyst, resulting in more NH_3 or NO being oxidized to N_2O.

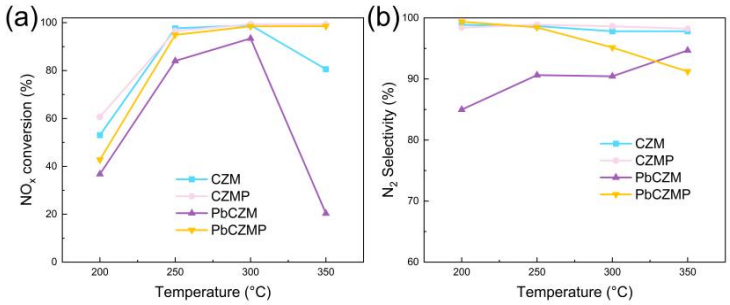

Figure. 2 (a) NOx conversion and (b) N_2 selectivity of catalysts before and after Pb poisoning.

3.3 Acid and redox site

NH_3-TPD is a common technique to analyze the strength and quantity of acidic sites of a material. The NH_3-TPD curves before and after Pb poisoning of these MCM-22 supported catalyst are shown in Fig. 3(a). The figure illustrates the desorption behavior of NH_3. The peak near 100 °C indicates the physical adsorption of NH_3, while the peak near 150 °C signifies the adsorption of NH_3 at the Bronsted acidic site. Additionally, the peaks near 300 °C depict the adsorption of NH_3 onto stronger Bronsted and Lewis acids.[8] It can be seen from the figure that the intensity of the 300 °C desorption peak in CZMP increased, indicating that phosphoric acid modification increased the Lewis acid site. However, the toxicity of the catalyst mainly inhibited the Bronsted acidic sites and Lewis acidic sites represented by the 150 °C desorption peak and the 300 °C desorption peak, which can be seen from the decrease of the area of the last two peaks in the TPD curve after poisoning, while the peak area of PbCZMP did not increase significantly. It can be found that the strong resistance of CZMP to Pb poisoning does not come from the increase of acidic sites.

H_2-TPR technique can qualitatively and quantitatively detect the content of oxides in the catalyst. Fig. 3(b) shows the H_2-TPR curves of catalysts before and after Pb poisoning. The reduction of CeO_2 results in three peaks in the curve. Among them, peaks 1, 2, and 3 could be assigned to the reduction of surface chemisorbed oxygen, surface Ce^{4+}, and bulk Ce^{4+}, respectively.[9] As illustrated in the figure, CZMP exhibits the highest adsorption of oxygen. This active adsorbed oxygen can combine with NO to form NO_2 and then undergo a rapid SCR reaction, thereby enhancing the catalytic performance of the catalyst.[10] This is a key factor contributing to the excellent low temperature performance of CZMP. Additionally, the reduction temperature of bulk phase Ce^{4+} in PbCZMP decreases, indicating that Ce^{4+} interacts with Pb, which is readily reduced to Ce^{3+}. This enhances the redox ability of the catalyst, resulting in a strong anti-poisoning capability.

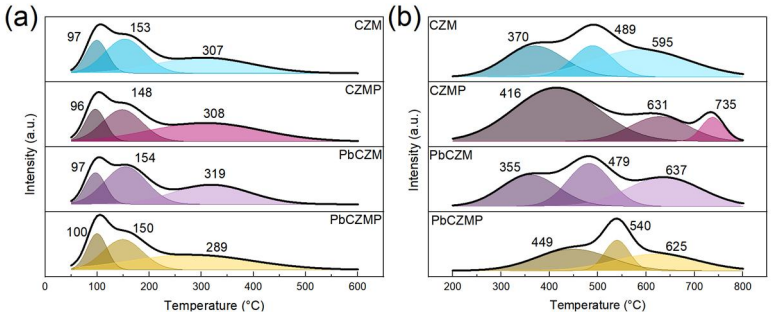

Figure. 3 (a) NH3-TPD and (b) H2-TPR curves of catalysts before and after Pb poisoning.

3.4 Reaction mechanism

The intermediates of NH_3-SCR reaction are very important for exploring the reaction mechanism. In-situ DRIFTs were used to study the adsorption and reaction of NH_3 and NO species of PbCZM and PbCZMP at 300 °C. According to other literatures and our previous studies, the peak groups, which located at about 3300 cm^{-1}, could be attributed to the N−H bonds from Lewis acid site in a formation of coordinated NH_3 species. While the peak at 1458 or 1460 cm^{-1} indicates that Bronsted acid sites with its NH^{4+} species were appeared on the catalyst. Additionally, the orange area in Fig. 4 represent the intermediates produced after adsorption NO such as nitrate species. The IR peak at 1538 (1510) cm^{-1} could be attributed to the a nitro substance produced by metals and nitrates such as monodentate nitrate, while the peak at 1570 cm^{-1} represents the combination of two metal sites and one nitrate to form bidentate nitrate. The peak at 1680 cm^{-1} indicated there are free NO_2 molecular which could carry out “fast SCR” reaction on the surface of PbCZMP. The IR spectra of the PbCZM and PbCZMP show a significant difference. For PbCZM, a large amount of NH_3 is present on the surface, indicating that the reaction is complete after only 15 minutes of NO penetration due to weak adsorption of NO. Similarly, PbCZMP also

exhibits a similar trend. However, the overall signal strength of PbCZMP is lower, suggesting that nitrate intermediates and free NO_2 molecules are highly active and can quickly decompose or combine with other substances to prevent their occupation of active sites. This suggests that the rapid degradation of these intermediates may be the key factor in the catalyst's strong resistance to Pb poisoning.

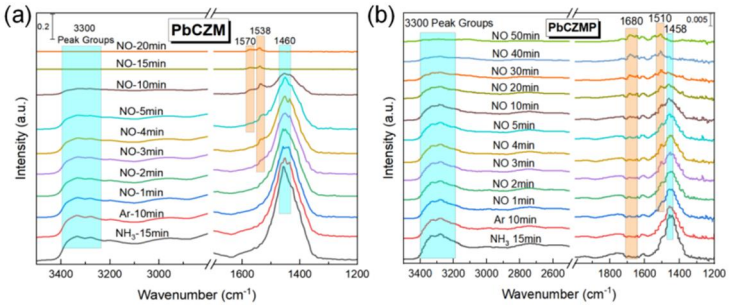

Figure. 4 In-situ DRIFT spectra of NO + O_2 adsorption with pre-adsorbed NH_3 at 300 ℃ over (a) PbCZM and (b) PbCZMP.

4. SUMMARY

In conclusion, the CeO_2-ZrO_2/MCM-22 catalyst treated with phosphoric acid exhibited outstanding NH_3-SCR performance at temperatures ranging from 200 to 350 °C. Moreover, the phosphoric acid modified catalyst also demonstrated superior resistance to Pb poisoning. XRD, FT-IR, and TEM results indicated that Pb poisoning did not destroy the phase or structure of the MCM-22 supported catalyst. Additionally, NH_3-TPD showed that phosphorylation could regulate the acidity of the catalyst, thus preventing Pb from occupying acidic sites. Furthermore, H_2-TPR indicated that strong oxidation capacity was a guarantee that the catalyst can still maintain excellent NH_3-SCR activity after being poisoned above 300 °C. Finally, in-situ DRIFTs revealed that after phosphoric acid modification, nitrate intermediates can be rapidly decomposed on the Pb-poisoned catalyst, thus improving the utilization rate of the active site.

5. ACKNOWLEDGMENTS

The authors wish to express their sincere appreciation for the financial support from Jiangxi Provincial Natural Science Foundation (20212BAB213032), National Natural Science Foundation of China (22072141, 52304429), Jiangxi Provincial Key Research and Development Program (20232BBG70012) and Engineering Research Center of Coal-based Ecological Carbon Sequestration Technology of the Ministry of Education (MJST2022-06).

6. REFERENCES

[1] Liu Mingxu, Shang Fang, Lu Xingjie, et al., Unexpected response of nitrogen deposition to nitrogen oxide controls and implications for land carbon sink, Nature Communications, 2022, 13(1): 3126.
[2] Liu Kaijie, Li Jingwei, Yu Qingbo, et al., Optimization and comprehensive mechanism of environment-friendly bimetal oxides catalysts for efficient removal of NO in ultra-low temperature flue gas, Separation and Purification Technology, 2023, 311: 123324.
[3] Yang Xin, Liu Kaijie, Han Xinyu, et al., Transformation of waste battery cathode material $LiMn_2O_4$ into efficient ultra-low temperature NH_3-SCR catalyst: Proton exchange synergistic vanadium modification, Journal of Hazardous Materials, 2023, 459: 132209.
[4] Jiang Ye, Gao Xiang, Zhang Yongxin, et al., Effects of $PbCl_2$ on selective catalytic reduction of NO with NH_3 over vanadia-based catalysts, Journal of Hazardous Materials, 2014, 274: 270-278.
[5] Jiang Ye, Liang Guitao, Bao Changzhong, et al., The poisoning effect of PbO and $PbCl_2$ on CeO_2-TiO_2 catalyst for selective catalytic reduction of NO with NH_3, Journal of Colloid and Interface Science, 2018, 528: 82-91.
[6] Zou Jingjing, Impeng Sarawoot, Wang Fuli, et al., Compensation or aggravation: Pb and SO_2 copoisoning effects over ceria-based catalysts for NOx reduction, Environmental Science & Technology, 2022, 56(18): 13368-13378.
[7] Jiang Ye, Yang Lin, Han Da, et al., The enhanced Pb resistance of CeO_2/TiO_2 catalyst for selective catalytic reduction of NO with NH_3 by the modification with W, Molecular Catalysis, 2021, 514: 111839.
[8] Han Xinyu, Bian Mengyao, Liu Kaijie, et al., Excellent MCM-49 supported CeCuOx nanocatalyst with ultrawide operating temperature window and strong anti-alkali ability for NH_3-SCR, ChemNanoMat, 2023, e202300407.

[9] Han Xinyu, Liu Kaijie, Bian Mengyao, et al., CeO2− δ nanoparticles supported on $SnNb_2O_6$ nanosheets for selective catalytic reduction of NOx with NH_3, ACS Applied Nano Materials, 2022, 5(9): 13529-13541.
[10] Lietti L., Forzatti P., Bregani F., Steady-state and transient reactivity study of TiO_2-supported V_2O_5-WO_3 De-NOx catalysts: Relevance of the vanadium-tungsten interaction on the catalytic activity, Industrial & Engineering Chemistry Research, 1996, 35(11): 3884-3892.